Numerical investigation of rubber swelling in bitumen

Wang, Haopeng; Liu, Xueyan; Apostolidis, Panos; Erkens, Sandra; Scarpas, Tom

DOI
10.1016/j.conbuildmat.2019.04.144

Publication date
2019

Document Version
Accepted author manuscript

Published in
Construction and Building Materials

Citation (APA)
Wang, H., Liu, X., Apostolidis, P., Erkens, S., & Scarpas, T. (2019). Numerical investigation of rubber swelling in bitumen. *Construction and Building Materials*, *214*, 506-515. https://doi.org/10.1016/j.conbuildmat.2019.04.144

Numerical Investigation of Rubber Swelling in Bitumen

Haopeng Wang[a*], Xueyan Liu[a], Panos Apostolidis[a], Sandra Erkens[a], Tom Scarpas[a,b]

[a] Section of Pavement Engineering, Faculty of Civil Engineering & Geosciences, Delft University of Technology, Delft, The Netherlands
[b] Department of Civil Infrastructure and Environmental Engineering, Khalifa University, Abu Dhabi, the United Arab Emirates

***Corresponding author**:
Email: haopeng.wang@tudelft.nl

ABSTRACT

Crumb rubber modified bitumen (CRMB) has been utilized in the asphalt paving industry for decades due to its various benefits. The main mechanisms of bitumen-crumb rubber interaction include rubber particle swelling and chemical degradation. Crumb rubber modifier (CRM) swelling plays a dominant role in controlling the property development of CRMB during the traditional interaction process. To have a better understanding of the swelling behavior of rubber in bitumen, this study developed a finite element model capable to simulate the multiphysics swelling phenomenon consisting of mass diffusion and volume expansion. The effects of various factors including material characteristics and process conditions on the rubber swelling in bitumen were investigated. The results indicate that the coupled diffusion-expansion model can predict the swelling behavior of rubber in bitumen. A good correlation between the simulation results and the previously reported evidences was observed. The effects of bitumen composition, rubber type and size, interaction temperature and time on swelling were successfully demonstrated by using the developed model with dedicated input parameters. With this study as a foundation, the estimated rubber swelling behavior in bitumen can be implemented into suitable micromechanical models to predict the viscoelastic properties of CRMB and consequently to optimize the design and process of bitumen-rubber blends.

Keywords: Crumb rubber modified bitumen; Swelling; Multiphysics; Diffusion; Finite Element Method

1. Introduction

According to the annual report of the European Tyre and Rubber Manufactures Association (ETRMA), it was estimated that in 2013, the European Union produced 3.6 million tonnes of end-of-life tires (ELTs) [1]. The rising environmental awareness and economic benefits have driven people to seek appropriate treatment and disposal of ELTs, such as retreading, energy recovery, pyrolysis and material recycling [2]. Among the material recycling methods, incorporating crumb rubber modifier (CRM) produced from scrap tires into bitumens has been widely utilized in the paving industry due to its tremendous economic and environmental benefits [3]. It was reported that crumb rubber modified bitumen (CRMB) can improve the overall performance of asphalt pavements, such as higher resistance to rutting, ageing, fatigue and thermal cracking [4]. This improvement significantly reduces the construction and maintenance cost of the pavement structures. In addition, rubberized asphalt pavement also has some intangible benefits, such as environmentally friendly disposal of scrap tires, increased skid resistance and noise reduction [5].

The bitumen-rubber interaction plays an important role not only in the development of CRMB properties but also, in its processing, storage and transport [4, 6, 7]. Depending on different interaction parameters (e.g., temperature, time and mixing technique, etc.), there are two mechanisms involved in the bitumen-rubber interaction process: rubber particles swelling and chemical degradation (devulcanization and/or depolymerization) [8, 9]. Based on the differences in polarity, bitumen molecules can be separated into four fractions, saturates, aromatics, resins and asphaltenes (SARA). Bitumen is commonly accepted as a multi-disperse colloidal system, where high-molecular-weight asphaltene micelles are peptized by resins and dispersed in low-molecular-weight maltenes (saturates and aromatics) [10]. In contrast, both natural and synthetic rubber used in tire manufacturing are high-molecular-weight macromolecules [11].

Figure 1 illustrates the different stages of bitumen-CRM interactions with increasing time at elevated temperatures. At stage 0, CRM particles are just immersed in bitumen matrix. Due to the thermodynamic compatibility between rubber and low-molecular-weight fractions of bitumen (maltenes) [12], maltenes diffuse into and are absorbed by the rubber networks. This causes the swelling of rubber particles and the formation of a gel-like structure adjacent to the bitumen-rubber interface (Stage 1). The swelling of CRM particles continues with the increasing interaction time. At a certain point, rubber swelling reaches its equilibrium with several times increase of the volume (Stage 2). After that, extending interaction time at elevated temperatures will result in rubber disintegration. CRM particles are split into smaller individuals due to the collapse of rubber network (Stage 3). When the interaction temperature is high enough, this process involves two chemical reactions: depolymerization and devulcanization [8], which break down the polymer chain bonds or crosslink bonds reducing thus the average molecular weight of rubber. It should be mentioned that the mixing energy exerted during the interaction process can accelerate the swelling and the size reduction of rubber particles. The degradation of rubber particles into the liquid phase of bitumen is detrimental to the development of mechanical properties of CRMB but beneficial to the storage stability [13]. However, at the traditional mixing temperatures of wet-processed rubberized binders (around 180°C), only partial degradation occurs, and the final binder properties are dominated by the CRM swelling process [8].

In general, CRM swelling has three effects on the properties of bitumen: (a) changing the component proportions due to absorption of maltenes; (b) changing the microstructure of bitumen; (c) stiffening the binder due to the inclusions of CRM particles with increased volume. Therefore, it is of vital importance to understand the swelling behavior of rubber to control the property development of CRMB. It was shown that the bitumen-CRM interactions and their effects on the final binder properties depend on the raw material parameters (e.g., bitumen characteristics, CRM type, morphology, particle size and dosage) and interaction conditions (e.g., mixing temperature, time and rate, energy type of the mechanical mixing exerted) [14-16]. Extensive laboratory tests have investigated the influence of these factors on the swelling behavior of CRM and on the properties of CRMB. Particularly, several dedicated studies were carried out to investigate the swelling behavior of individual rubber block or sheet in hot bitumen [12, 17, 18]. However, these laboratory tests are always time and cost consuming. In addition, the findings from the laboratory tests are highly dependent on the combinations of materials and processing methods, which are lack of universality. Based

on their findings, it is generally assumed that the swelling of CRM in bitumen is a diffusion induced process with volume expansion. A numerical approach through a simplified system can provide a convenient way to quickly identify the parameters that affect the swelling process and hence can be used to perform a preliminary evaluation before the experimental tests.

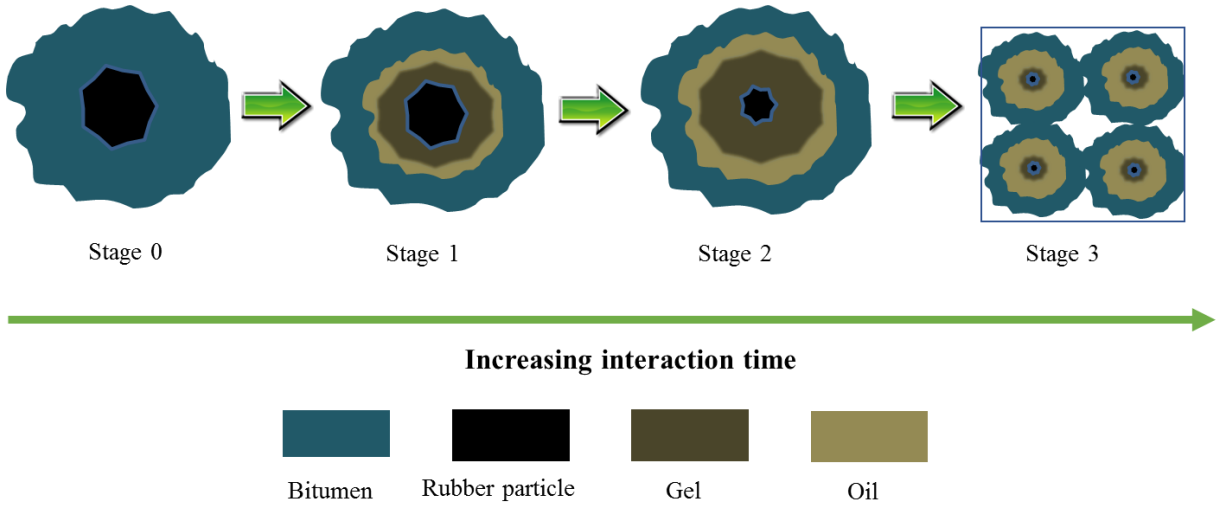

Figure 1. Schematic representation of the bitumen-rubber interaction process.

2. Objective

To have a better understanding of the swelling behavior of rubber in bitumen, this study aims to develop a modeling methodology capable to simulate the rubber swelling process in bitumen. The mass diffusion and volume expansion phenomena of the rubber are incorporated in a multi-physics tool to predict the rubber swelling in bitumen. The model is calibrated with data generated from previous studies proving the reliability of the tool to evaluate the various influential factors on the design of rubberized bituminous materials with the desired properties and subsequently performance.

3. Multiphysics modeling of the swelling behavior of rubber in bitumen

From the physical viewpoint, rubber swelling is a multiphysics phenomenon which consists of mass diffusion and volume expansion (mechanical deformation) [19]. Numerical modeling of rubber swelling will provide new insights into the mechanical mechanism of it. This section presents the theory for mass diffusion and large deformations based on the balance equations driving the solvent diffusion and the force equilibrium, and the constitutive equations for rubber particles.

3.1. Mass Diffusion

As reported by many studies, it is the maltenes in bitumen that diffuse into the rubber network due to the similar solubility parameters between aromatics and rubber [12]. As shown in Figure 2, the driving force of the diffusion process is the chemical potential of the external solvent (maltenes) produced from the concentration difference between rubber and bitumen [20]. This diffusion process continues until the concentrations of light fractions inside and outside the rubber are uniform and, consequently, equilibrium swelling is reached. Fick's law of diffusion is usually used to describe the kinetics of bitumen diffusion into rubber. Fick's first law postulates that the diffusive flux goes from regions of high concentration to regions of low concentration, with a magnitude that is proportional to the concentration gradient measured normal to the section:

$$\boldsymbol{J} = -D\nabla C \tag{1}$$

where $\boldsymbol{J}$ is the diffusion flux vector; D is the diffusion coefficient, which is assumed to be constant; C is the concentration; ∇ is the nabla operator or gradient operator. Fick's second law predicts how diffusion causes the concentration to change with time given as

$$\frac{\partial C}{\partial t} = D\nabla^2 C \tag{2}$$

where t is time; other parameters are the same as Equation 1. The flux vector is associated with the mass balance equation above and imposed at the boundary conditions of the rubber domain.

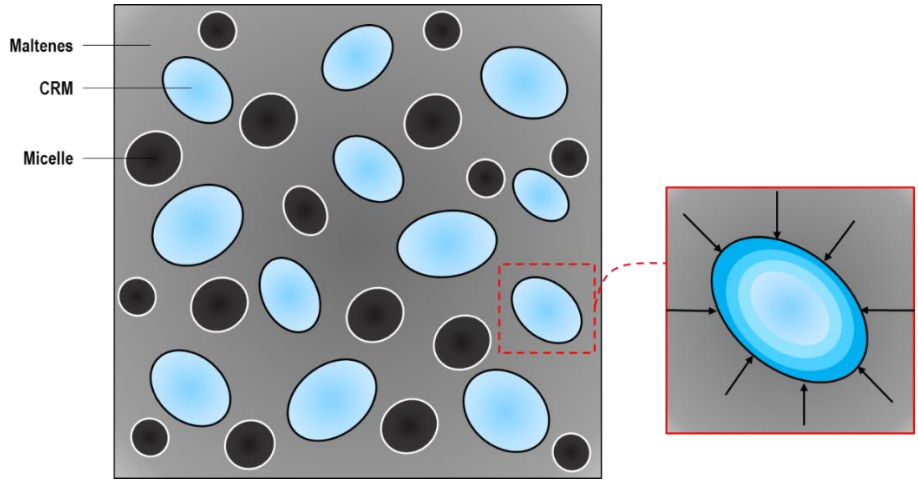

Figure 2. Schematic representation of maltenes diffusion into rubber.

3.2. Volume Expansion

The volume expansion of rubber can be treated as a large deformation problem. Rubber particle is considered as a homogenized continuum body. In principle, the equations that govern the mechanics of rubber particles during swelling include balance equations, kinematic equations and constitutive equations [21]. The equilibrium equation of the system is given by Newton's second law ($\sum F = ma$). Considering both force and area are represented in the material configuration, the equation of motion can be written as

$$\nabla \cdot \mathbf{FS} + \mathbf{F_v} = 0 \tag{3}$$

where $\mathbf{F}$ is the deformation gradient tensor; $\mathbf{S}$ is the second Piola-Kirchhoff stress; $\mathbf{F_v}$ is the volume force vector. The deformation tensor $\mathbf{F}$ is defined in terms of displacement gradient as:

$$\mathbf{F} = \nabla\mathbf{u} + \mathbf{I} \tag{4}$$

where $\mathbf{u}$ is the displacement; $\mathbf{I}$ is the identity tensor. In geometrically nonlinear analysis, the stress should in general be interpreted as second Piola-Kirchhoff stress. The Lagrange-Green strain tensor $\mathbf{E}$ is related to displacement by:

$$\mathbf{E} = \frac{1}{2}\left(\mathbf{F}^{\mathbf{T}}\mathbf{F} - \mathbf{I}\right) = \frac{1}{2}\left[\nabla\mathbf{u} + (\nabla\mathbf{u})^{\mathbf{T}} + (\nabla\mathbf{u})^{\mathbf{T}}\nabla\mathbf{u}\right] \tag{5}$$

To include the notion of material inelastic deformation into a large deformation framework, the following multiplicative decomposition of the total deformation gradient tensor $\mathbf{F}$ is proposed:

$$\mathbf{F} = \mathbf{F}_{\text{el}}\mathbf{F}_{\text{inel}} \tag{6}$$

where $\mathbf{F}_{\mathrm{el}}$ is the undamaged elastic deformation tensor; $\mathbf{F}_{\mathrm{inel}}$ is the inelastic deformation tensor. Furthermore, the undamaged elastic deformation gradient can be written as:

$$\mathbf{F}_{\mathrm{el}} = \mathbf{F}\mathbf{F}_{\mathrm{inel}}^{-1} \tag{7}$$

In this study, the initial strain was considered as zero and the inelastic strain refers only to the swelling strain. The elastic Lagrange-Green strain tensor is then computed as:

$$\mathbf{E}_{\mathrm{el}} = \frac{1}{2}\left(\mathbf{F}_{\mathrm{el}}{}^{\mathrm{T}}\mathbf{F}_{\mathrm{el}} - \mathbf{I}\right) \tag{8}$$

The constitutive equation for a linear elastic material relates the stress tensor to the elastic strain tensor.

$$\boldsymbol{\sigma} = \mathbf{C}\colon \mathbf{E}_{\mathrm{el}} \tag{9}$$

Here, the Cauchy stress tensor $\boldsymbol{\sigma}$ and strain tensor $\mathbf{E}_{\mathrm{el}}$ are second-order tensor, while the constitutive elasticity tensor $\mathbf{C}$ is a fourth-order tensor. With the relationship between Cauchy stress and second Piola-Kirchhoff stress,

$$\boldsymbol{\sigma} = J^{-1}\mathbf{F}\mathbf{S}\mathbf{F}^{\mathrm{T}} \tag{10}$$

where J is the determinant of deformation tensor, the constitutive equation for the elastic rubber can be written as:

$$\mathbf{S} = J_{\mathrm{in}}\mathbf{F}_{\mathrm{inel}}^{-\mathrm{T}}(\mathbf{C}\colon \mathbf{E}_{\mathrm{el}})\mathbf{F}_{\mathrm{inel}}^{-1} \tag{11}$$

3.3. Multiphysics Coupling

Rubber swelling creates an inelastic strain that is proportional to the difference between the concentration and the strain-free reference concentration:

$$\boldsymbol{\varepsilon}_s = \boldsymbol{\beta}_{\mathrm{s}} c_{\mathrm{diff}} \tag{12}$$

where $\boldsymbol{\varepsilon}_s$ is the inelastic strain caused by swelling; c_{diff} is the concentration difference; $\boldsymbol{\beta}_{\mathrm{s}}$ is the coefficient of swelling, the coefficient of swelling is a second-order tensor, which can be defined as isotropic, diagonal, or symmetric. In this case, the coefficient of swelling is isotropic, so only uniform volumetric expansion is taken into account. Since swelling strain is assumed to be the only contribution to the inelastic strain in this case (Equation 13),

$$\mathbf{F}_{\mathrm{inel}} = {J_s}^{1/3}\mathbf{I} \tag{13}$$

the total deformation gradient tensor $\mathbf{F}$ is scaled by the swelling stretch to form the elastic deformation gradient tensor $\mathbf{F}_{\mathrm{el}}$:

$$\mathbf{F}_{\mathrm{el}} = \mathbf{F}{J_s}^{-1/3} \tag{14}$$

where J_s is the swelling ratio (volumetric expansion ratio) or the determinant of inelastic deformation tensor, and it relates to swelling strain as:

$$J_s = (1 + \varepsilon_s)^3 = (1 + \beta_{\mathrm{s}} c_{\mathrm{diff}})^3 \tag{15}$$

As swelling process consists of mass diffusion and volume expansion, it induces a one-way coupling between concentration and mechanics. In general, the maltenes concentration within the rubber is unknown and has to be computed with a preceding simulation with known material parameters. Therefore, the concentration is calculated in a first time-dependent study in the mass transport domain, and then the structural domains are computed in a stationary study based on the results obtained from transport domain.

This sequential approach will significantly reduce the computation time compared to a single solution including all physical interfaces.

4. Finite element model

4.1. Model Definitions

The coupled diffusion-expansion model described in the previous section was implemented in the finite element software COMSOL Multiphysics. The numerical simulations were performed on a square two-dimensional domain of 1.0 × 1.0 mm meshed with triangular elements. This domain represented the typical microscopic images of CRMB considering the real sizes of rubber particles. To simplify the model, the rubber particle was assumed to be a homogenous isotropic sphere embedded in the bitumen matrix. The complete geometry and mesh of a single rubber particle are shown in Figure 3a. The diameter of the single rubber particle was set as 0.3 mm. In terms of the boundary conditions (Figure3b), the left and bottom sides of the domain were set as symmetrical in which the two boundaries are free to move along directions paralleled to its boundary plan respectively. The right and top sides of the domain were set as free in term of displacement and no influx imposed. The free boundary conditions of right and top were set to demonstrate the volume expansion visually by the movement of bitumen matrix. In order to directly visualize the effect of rubber particle size on swelling, another finite element model consisting of five rubber particles with varying diameters (0.2, 0.4, 0.6, 0.8, 1.0 mm) was also developed as shown in Figure 4a. The boundary conditions (Figure 4b) were set similar as the single rubber particle model except that the top and right sides of the domain were set as fixed boundaries in the structural domain tosimulate the real mixing scenario by considering the constraints from the vessel. The interparticle effect (interference) on the rubber swelling can also be demonstrated by this case. The initial solvent concentration within the rubber was set as zero, which is the strain-free reference concentration. The periphery boundaries of the rubber particle contacted directly to the bitumen was set to have the same concentration as the surrounding bitumen matrix. The swelling process of different-size rubber particles in bitumen with different SARA fractions at various interaction conditions were simulated on the basis of the proposed coupled diffusion-expansion model.

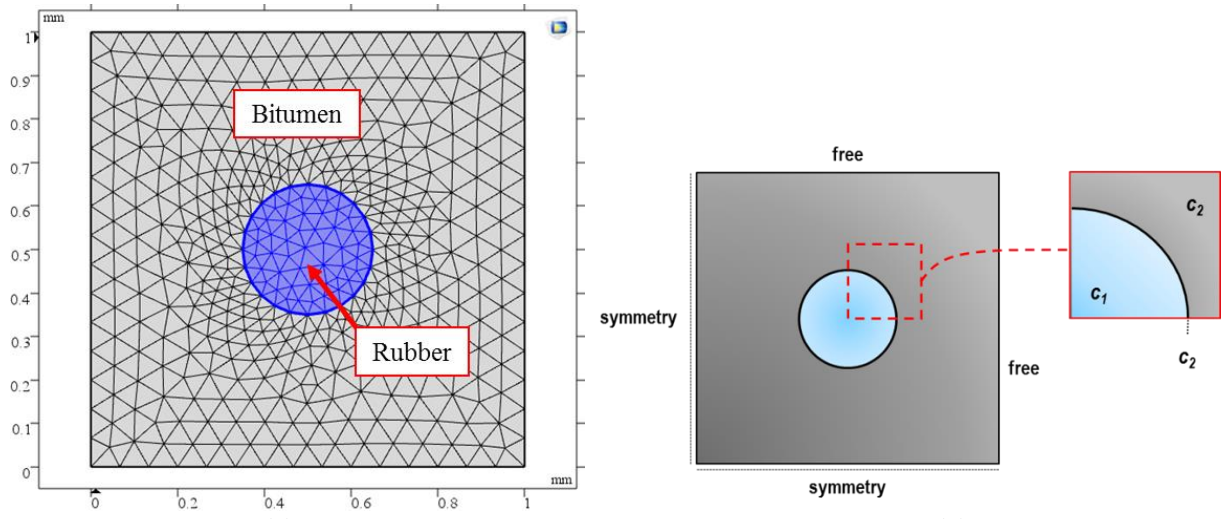

(a) **(b)**

Figure 3. (a) Geometry and mesh of the modelling domain: single rubber particle; (b) Schematic of boundary conditions.

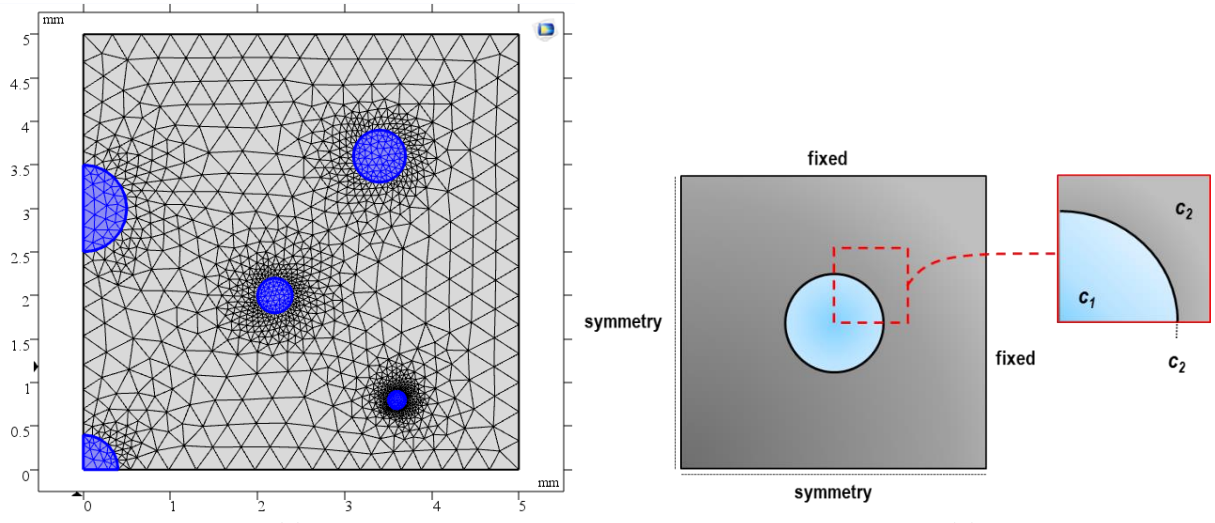

(a) (b)

Figure 4. (a) Geometry and mesh of the modelling domain: multiple rubber particles of varying sizes; (b) Schematic of boundary conditions.

4.2. Input Parameters and Model Validation

The parameters used in the modeling were determined and collected from published literatures. To investigate the effects of various factors (e.g., bitumen composition, CRM type and size, interaction temperature and time) on the swelling behaviors, four types of bitumen with 50 and 100 penetration grades of Kuwaiti (KSR) and Venezuelan (VEN) origins, car tire rubber and truck tire rubber were employed to interact at three different temperatures, 150, 180 and 210 °C, respectively. The simulated cases in this study were based on the research conducted by Artamendi and Khalid [12] and were compared with the experimental results. Laboratory tests of rubber swelling in bitumen were conducted by immersing weighed rubber samples in bitumen at elevated temperatures. Rubber samples were periodically taken out and reweighed, through which the mass uptake was obtained by the difference between the initial weight and the weight after immersion in bitumen. Based on the laboratory tests, the related parameters, such as equilibrium concentration, diffusion coefficient and swelling coefficient, were calculated. The equilibrium concentration and diffusion coefficient were offered in the original paper. The swelling coefficient was calculated by dividing the swelling strain by the concentration difference in Equation 12. By defining different values for the material property parameters, the simulation cases listed in Table 1 were numerically implemented in the model. The density of bitumen was set as 0.93 g/cm^3 at high temperatures. The rubber particle was set to have a density of 1 g/cm^3, a Young's modulus of 8 MPa, and a Poisson's ratio of 0.45. Based on the experimental results, it was found that the swelling coefficients of rubber at different temperatures for given materials are close to each other. However, the diffusion coefficients are highly temperature dependent.

Table 1. Material parameters used in the simulation

Case	Bitumen type	SARA fractions (%)	Temperature (°C)	Rubber source	Equilibrium concentration (kg/m^3)	Diffusion coefficient, D (m^2/s)	Swelling coefficient, β_s (m^3/kg)
1	100KSR	7.1+57.6+19.1+16.2	150	Car tire	399.4	1.31×10^{-11}	4.85×10^{-4}
2				Truck tire	523.9	1.69×10^{-11}	5.73×10^{-4}
3			180	Car tire	399.4	1.96×10^{-11}	4.85×10^{-4}
4				Truck tire	523.9	2.61×10^{-11}	5.73×10^{-4}
5			210	Car tire	399.4	5.86×10^{-11}	4.85×10^{-4}
6				Truck tire	523.9	6.77×10^{-11}	5.73×10^{-4}

7	50KSR	8.0+48.0+22.0+22.0	180	Car tire	415.2	1.96×10^{-11}	4.95×10^{-4}
8			180	Truck tire	469.9	2.15×10^{-11}	5.30×10^{-4}
9	100VEN	9.7+49.8+23.5+17.0	180	Car tire	457.4	7.11×10^{-11}	5.22×10^{-4}
10			180	Truck tire	558.8	7.42×10^{-11}	6.06×10^{-4}
11	50VEN	8.0+51.4+19.7+20.9	180	Car tire	430.1	3.37×10^{-11}	5.03×10^{-4}
12			180	Truck tire	469.9	3.82×10^{-11}	5.30×10^{-4}

Model validation is concerned with quantifying the accuracy of the model by comparing numerical solutions to experimental data. To validate the developed swelling model, the simulation of rubber swelling in 100KSR bitumen at 180 °C (case 3 and 4) were taken as an example and the simulation results were compared with the experimental data [12]. For the case of one-dimensional diffusion, the analytical solution of Fick's laws for shorter times is shown in Equation 16 [22].

$$\frac{M_t}{M_\infty} = \frac{4}{d}\sqrt{\frac{Dt}{\pi}} \quad (16)$$

where M_t and M_∞ are the masses of the diffusing substance absorbed at time t and at equilibrium respectively; t is the immersion time (s) for the rubber in bitumen and d is the rubber sample thickness (mm). This equation indicates a linear relationship between initial weight gain ($M_t/M_\infty < 0.6$) and the square root of time.

Figure 5 shows the variation in M_t/M_∞ with $t^{1/2}/d$ for the absorption of 100KSR bitumen into truck and car tire rubber at 180 °C. Both experimental and numerical data in Figure 5 verify the linear regions in the early stages of diffusion for both types of rubber. It can be seen from Figure 4 the numerical data correlates well with the experimental data. In addition, truck-tire rubber reaches the equilibrium earlier than car-tire rubber does. This finding is consistent with the experimental results and is because truck-tire rubber contains more natural rubber which swells faster than synthetic rubber in bitumen.

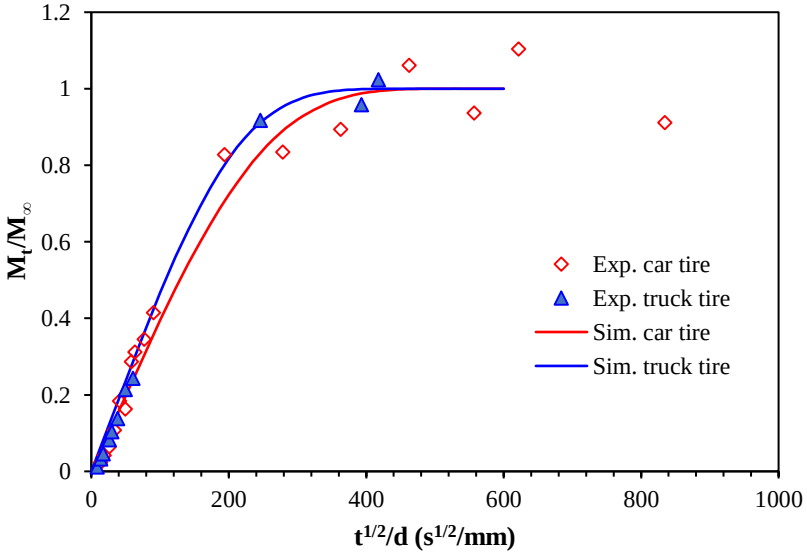

Figure 5. Bitumen absorption into rubber at 180 °C during the swelling process.

Figure 6a presents the total displacement contour of rubber particle in bitumen when equilibrium swelling reaches for Case 3 and 4 simulations. The maximum displacements for two cases were also annotated in the figure. It can be found that car-tire rubber produces less swelling than truck-tire rubber under the same condition. Truck-tire rubber contains more natural rubber components, which are more prone

to swell in bitumen due to the high chain flexibility of simple long-chain structure with less network constraints comparing to the synthetic rubber in car-tire rubber. It is noteworthy that, due to the swelling of rubber in bitumen, bitumen matrix was squeezed out of the original boundary. In addition, the swelling of rubber is not uniform due to the constraints of surrounding bitumen. To calculate the volume change (area change in 2D model) of rubber during swelling, deformed geometries were generated as shown in Figure 6b. The black circle represents the original rubber particle while the red one represents the swollen rubber particle. The area of swollen rubber particle was calculated using the surface integral based on the deformed geometry. The volume change of rubber particles during the swelling process were illustrated in terms of swelling ratio in Figure 6c. The swelling ratio was defined as the area increase divided by the original area of rubber particle. It can be seen from Figure 6c that swelling of rubber happens faster at the earlier stage of interaction, which is consistent with the diffusion process. With the increase of interaction time, car-tire and truck-tire rubber sequentially reached the swelling equilibrium at 1150 s and 900 s, respectively. The equilibrium times from simulation are close to the experimental counterparts, 1014 s and 762 s. As expected, truck-tire rubber has a larger equilibrium swelling ratio in bitumen than car-tire rubber. For the case of 100KSR bitumen at 180 °C, the equilibrium swelling extent for car-tire and truck-tire rubber was 0.49 and 0.79, respectively.

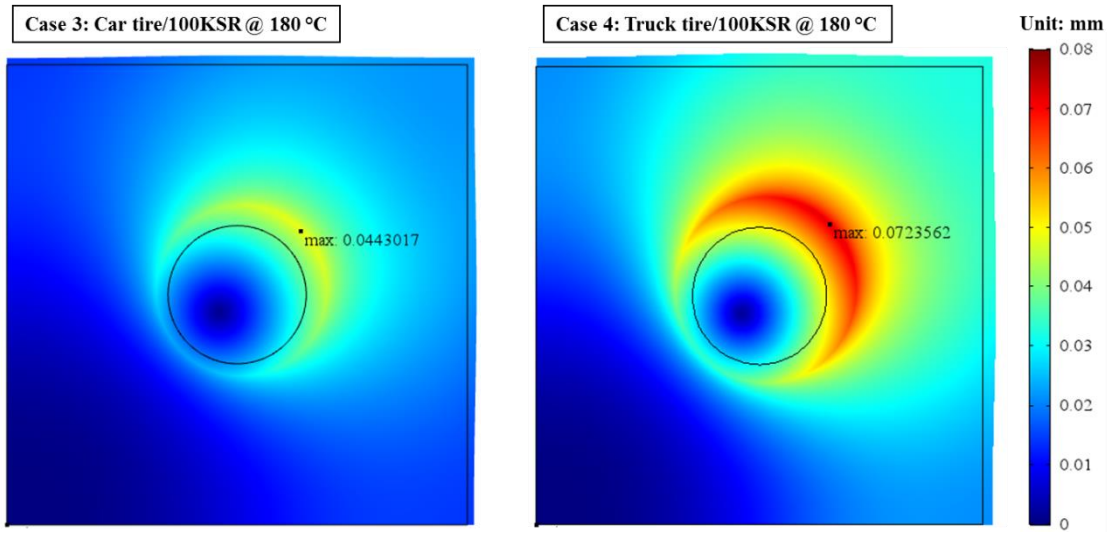

(a)

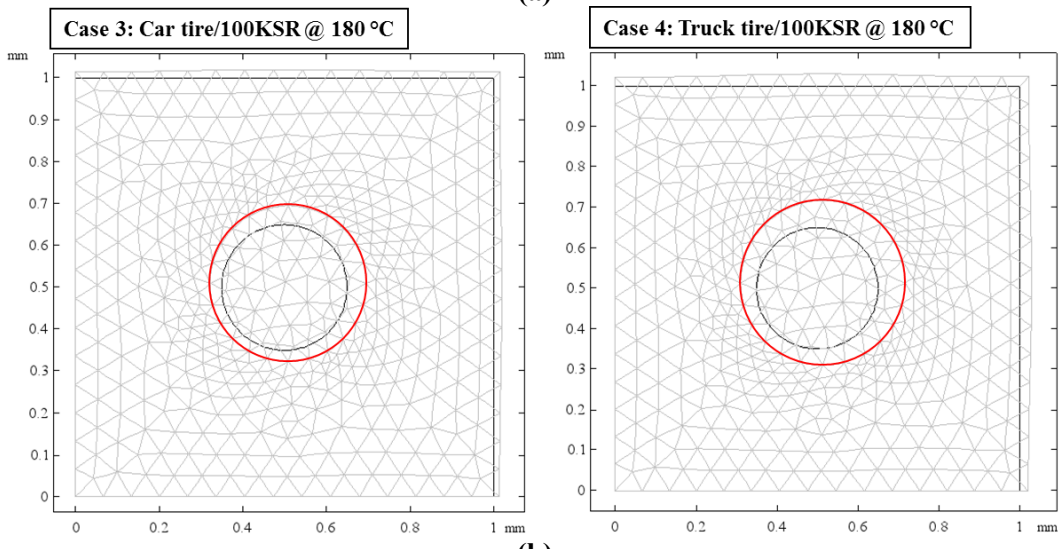

(b)

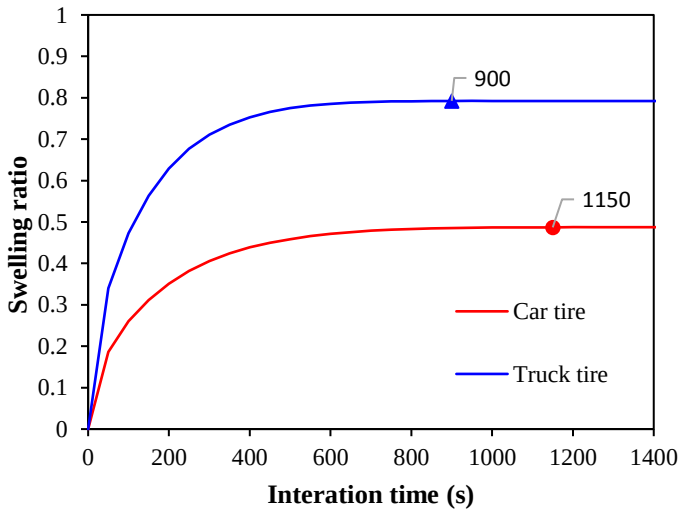

(c)

Figure 6. Simulation results for Case 3 and 4: (a) total displacement of rubber particle in bitumen at the equilibrium swelling state; (b) deformed mesh of the model at the equilibrium swelling state; (c) volume change of rubber particles during swelling

5. Results and discussions

5.1. Effect of Temperature on Swelling

The simulation results for Case 1-6 were summarized in Figure 7 in terms of variation in swelling ratio with interaction time. For both car-tire and truck-tire rubber, with the increase of interaction temperature, swelling of rubber particles in bitumen takes place faster. The higher the interaction temperature, the shorter time rubber particles need to reach the equilibrium. This is because of the increased diffusion coefficients at increased temperatures which stems from the greater segmental motion of polymer chains. In general, the equilibrium swelling ratio of rubber at different temperatures are identical. The simulation results exactly correspond to the experimental data. Some studies also found that as the temperature increases, the rate of swelling increases and the swelling extend decreases [8]. This contradictory result maybe stems from the partial dissolution of rubber into bitumen at elevated temperatures. The measured mass uptake and hence swelling ratio was smaller than expected due to the loss of the sample integrity.

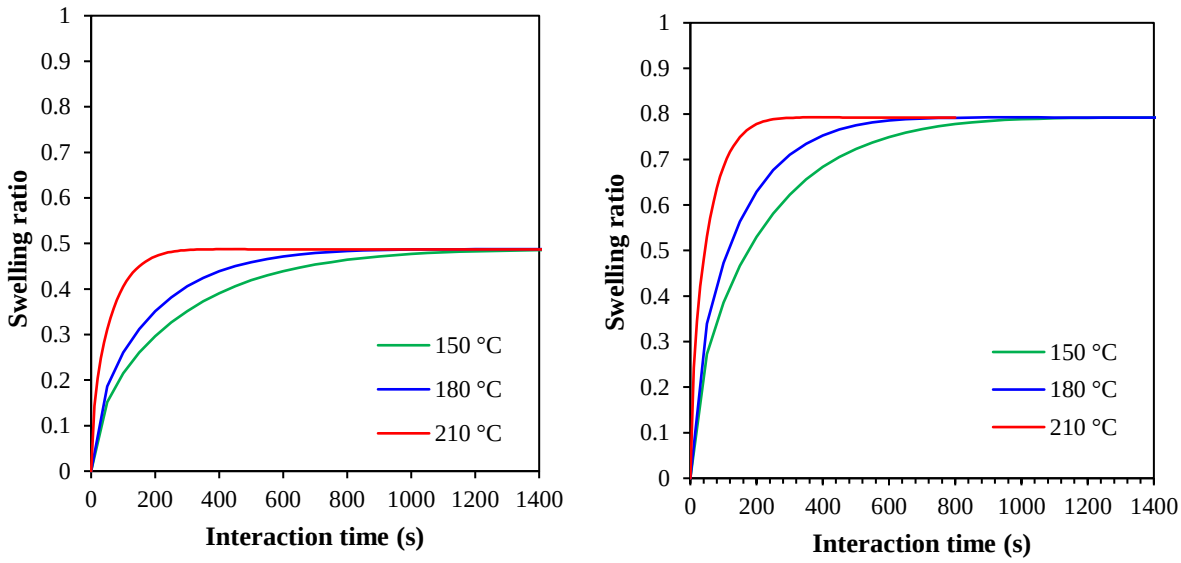

Figure 7. Rubber swelling in KSR100 bitumen at different temperatures: (a) car tire; (b) truck tire.

5.2. Effect of Bitumen Composition on Swelling

The different crude oil sources and diverse fuel processing technologies produce various chemistry of bitumen, specifically with various SARA fractions, and consequently influence the compatibility with CRM and the rubber swelling development in bitumen. The simulation results for demonstrating the effect of bitumen composition on swelling were summarized in Figure 8 in terms of variation in swelling ratio with interaction time. It can be seen from Figure 8 that even in the same grade bitumen from different origins, rubber particles swell differently. For the same grade bitumen, both car-tire and truck-tire rubber particles seems to be more prone to swell in the Venezuelan bitumen than the Kuwaiti. In addition, within each bitumen type, rubber can swell faster and more in the high penetration grade bitumen, which correspond to the bitumen with higher maltenes content and lower asphaltene content. This is because the aromatic fractions (maltenes) of bitumen have similar solubility parameters with rubber and therefore better compatibility [10]. Asphaltenes have high molecular weight and are not likely to diffuse into the rubber network and make it swell.

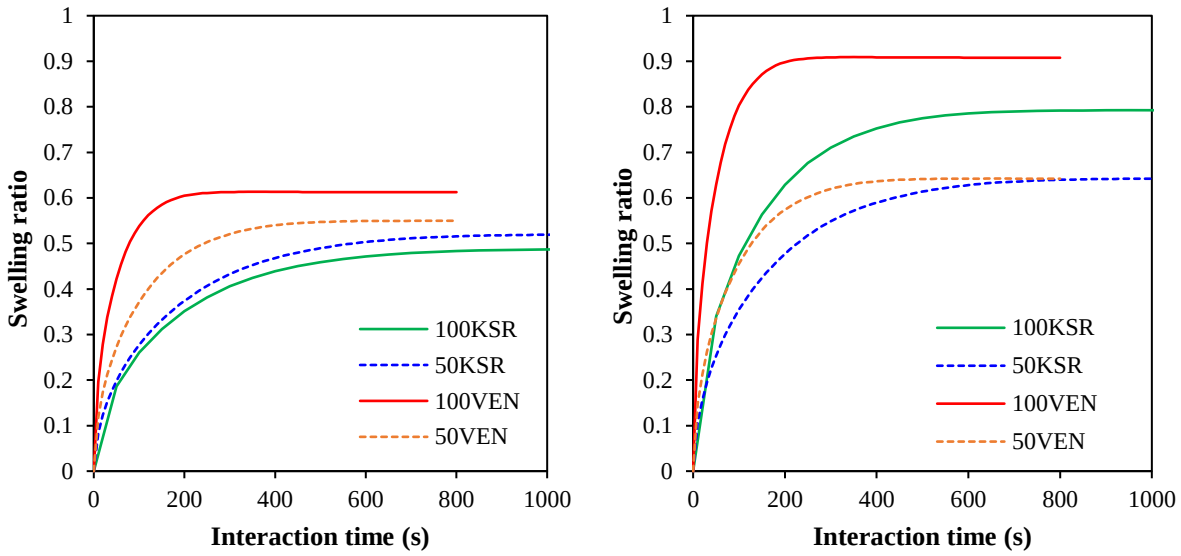

Figure 8. Rubber swelling in different bitumens at 180 °C: (a) car tire, (b) truck tire.

5.3. Effect of Rubber Particle Size on Swelling

As shown in Figure 4a, a separate model geometry which involved five rubber particles with varying diameters (0.2, 0.4, 0.6, 0.8, 1.0 mm) was also developed to investigate the effect of particle size on swelling. The input material parameters for Case 3 were applied for this specific simulation. Figure 9 presents the simulation results of swelling of rubber particles with different sizes. It can be seen from Figure 9a that small rubber particles (with diameter of 0.2 and 0.4 mm) are fully saturated with maltenes at t=1800 s while other particles still have a concentration gradient along the direction from outer to inner. The particle size has influence on the time-dependent diffusion process and further affects the swelling behavior of rubber. It is understandable that large rubber particles have larger volume changes after the same interaction time as shown in Figure 9b. However, small rubber particles swell faster and reach the equilibrium swelling at an earlier stage than big particles do as shown in Figure 9c. The asymmetric displacement of a certain rubber particle is due to the interference effect from neighbor particles, which creates extra forces on the rubber particles. Since the input material parameters for the rubber particles are identical, it is predictable that rubber particles with varying sizes will have the same swelling ratio when equilibrium swelling reaches. The only difference is that big rubber particles need longer time to reach the equilibrium. This is also can be explained by Equation 16 that if considering swelling as a Fickian diffusion process, the required interaction time to achieve the same swelling ratio increases with the square of the particle size.

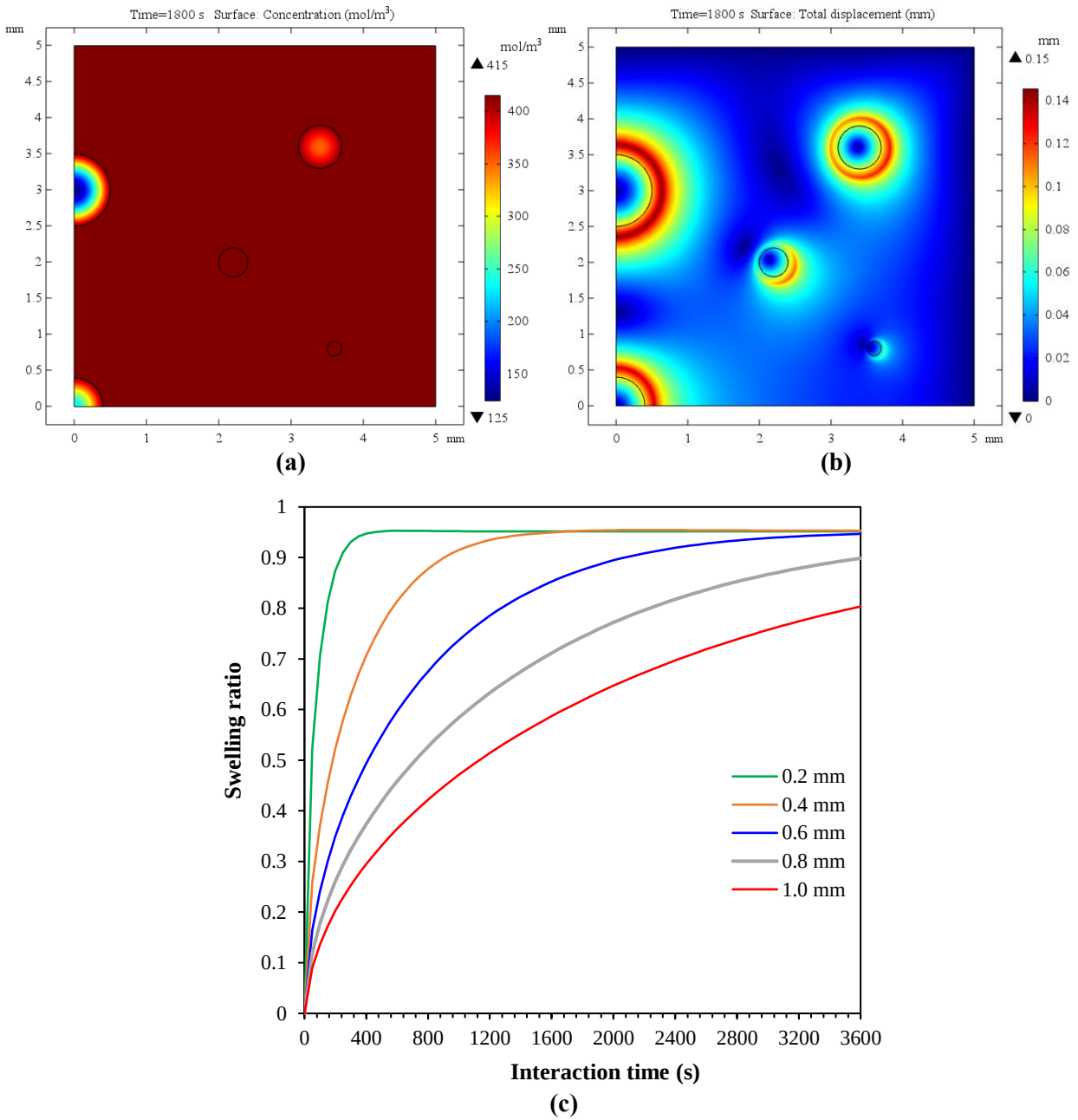

Figure 9. Rubber particles of varying sizes swelling in bitumen at 180 °C: (a) concentration at t=1800 s; (b) total displacement of rubber particles at t=1800 s; (c) variation in swelling ratio with time.

5.4. Potential application

The inclusion of CRMs in bitumen stiffens the binder. Such a modified bitumen is similar to particulate filled polymer matrix composites. Comparing to the rigid mineral filler in asphalt mastics, the stiffening or reinforcement mechanisms of CRMs in bitumen may include volume-filling reinforcement, physiochemical reinforcement and particle-interaction reinforcement [23, 24]. The effective viscoelastic behavior of CRMB can be predicted by particulate composite micromechanical models addressing the above reinforcement mechanisms. The micromechanical models are generally based on the mechanical properties and volume fractions of individual constituents [25]. The importance of estimating the swelling of CRMs in bitumen is

that if known, then it may be possible to use suitable micromechanical models with some level of accuracy to estimate the viscoelastic properties of CRMB. With the predicted properties of CRMB, it might be possible to optimize the design and process of bitumen-rubber blends and to set quality control limits to ensure a well-performing mixture.

6. Conclusions

With the aim of predicting the swelling behavior of rubber in bitumen, this study presented a coupled diffusion-expansion model to address the multiphysics of swelling which consists of mass diffusion and volume expansion. In this model, a one-way coupling was introduced between concentration and mechanics. Firstly, the mass concentration is calculated in a time-dependent study in the mass transport domain, and then the structural domains are computed in a stationary study based on the results got from transport domain. Based on the numerical simulation results, the following conclusions can be drawn:

- There is a good correlation between the simulation results and the previously reported experimental results. The developed model can effectively predict the swelling behavior of rubber in bitumen.
- Under the same condition, truck-tire rubber can absorb more bitumen and cause more swelling than car-tire rubber. For instance, for the case of rubber swelling in 100KSR bitumen at 180 °C, the equilibrium swelling ratio for car-tire and truck-tire rubber was 0.49 and 0.79, respectively.
- Temperature is a crucial factor affecting the swelling process. With the increase of temperature, the diffusion coefficient increases and the equilibrium swelling time decreases.
- In general, high penetration grade bitumen with higher aromatic fractions is more compatible with rubber and therefore increases the swelling extent of rubber.
- Under the same condition, small rubber particles swell faster and reach the equilibrium swelling at an earlier stage than large rubber particles.

The developed multiphysics model creates an opportunity to apply the estimated swelling behaviors of rubber into suitable micromechanical model for further property predictions of CRMB. Further dedicated experimental studies are recommended to be conducted to establish a database of the material properties of various rubbers and bitumens to serve as the input parameters in the developed model. The effects of geometry and distribution (interparticle interaction) of rubber particles on the swelling development are also challenging.

Acknowledgements

The corresponding author would like to thank the financial support from China Scholarship Council.

References

[1] ETRMA. End-of-life Tyre Report 2015. Brussels: European Tyre & Rubber Manufacturers' Association; 2016.

[2] Sienkiewicz M, Kucinska-Lipka J, Janik H, Balas A. Progress in used tyres management in the European Union: a review. Waste Manag. 2012;32(10):1742-51.

[3] Wang T, Xiao F, Zhu X, Huang B, Wang J, Amirkhanian S. Energy consumption and environmental impact of rubberized asphalt pavement. Journal of Cleaner Production. 2018;180:139-58.

[4] Lo Presti D. Recycled Tyre Rubber Modified Bitumens for road asphalt mixtures: A literature review. Construction and Building Materials. 2013;49:863-81.

[5] Wang H, Liu X, Apostolidis P, Scarpas T. Review of warm mix rubberized asphalt concrete: Towards a sustainable paving technology. Journal of Cleaner Production. 2018;177:302-14.

[6] Wang H, Liu X, Apostolidis P, Scarpas T. Rheological Behavior and Its Chemical Interpretation of Crumb Rubber Modified Asphalt Containing Warm-Mix Additives. Transportation Research Record: Journal of the Transportation Research Board. 2018.

[7] Wang H, Liu X, Apostolidis P, Scarpas T. Non-Newtonian Behaviors of Crumb Rubber-Modified Bituminous Binders. Applied Sciences. 2018;8(10):1760.
[8] Abdelrahman MA, Carpenter SH. Mechanism of the interaction of asphalt cement with crumb rubber modifier. Transportation Research Record: Journal of the Transportation Research Board. 1999;1661:106-13.
[9] Wang H, Liu X, Zhang H, Apostolidis P, Scarpas T, Erkens S. Asphalt-rubber interaction and performance evaluation of rubberised asphalt binders containing non-foaming warm-mix additives. Road Materials and Pavement Design. 2018:1-22.
[10] Lesueur D. The colloidal structure of bitumen: consequences on the rheology and on the mechanisms of bitumen modification. Advances in colloid and interface science. 2009;145(1-2):42-82.
[11] Mark JE, Erman B, Roland M. The science and technology of rubber: Academic press; 2013.
[12] Artamendi I, Khalid HA. Diffusion kinetics of bitumen into waste tyre rubber. Journal of the Association of Asphalt Paving Technologists. 2006;75:133-64.
[13] Ghavibazoo A, Abdelrahman M, Ragab M. Mechanism of Crumb Rubber Modifier Dissolution into Asphalt Matrix and Its Effect on Final Physical Properties of Crumb Rubber-Modified Binder. Transportation Research Record: Journal of the Transportation Research Board. 2013(2370):92-101.
[14] Shen J, Amirkhanian S. The influence of crumb rubber modifier (CRM) microstructures on the high temperature properties of CRM binders. International Journal of Pavement Engineering. 2007;6(4):265-71.
[15] Abdelrahman M. Controlling performance of crumb rubber-modified binders through addition of polymer modifiers. Transportation Research Record: Journal of the Transportation Research Board. 2006(1962):64-70.
[16] Airey G, Rahman M, Collop AC. Crumb Rubber and Bitumen Interaction as a Function of Crude Source and Bitumen Viscosity. Road Materials and Pavement Design. 2004;5(4):453-75.
[17] Frantzis P. Crumb rubber-bitumen interactions: Diffusion of bitumen into rubber. Journal of materials in civil engineering. 2004;16(4):387-90.
[18] Feng W, Minming K, Guanlong L, Xiaolong Z, Chenglie L. Investigation of Swelling and Dissolution Process of Natural Rubber in Aromatic Oil. China Petroleum and Petrochemical Technology. 2015;17:76-86.
[19] Wang H, Apostolidis P, Liu X, Scarpas T. Modeling of rubber swelling in bituminous binders. Advances in Materials and Pavement Prediction: Papers from the International Conference on Advances in Materials and Pavement Performance Prediction (AM3P 2018), April 16-18, 2018, Doha, Qatar: CRC Press; 2018. p. 181.
[20] Frantzis P. Crumb rubber-bitumen interactions: Cold-stage optical microscopy. Journal of Materials in Civil Engineering. 2003;15(5):419-26.
[21] Scarpas A. A mechanics based computational platform for pavement engineering. Delft, The Netherlands: Delft University of Technology; 2004.
[22] Crank J. The Mathematics of Diffusion. Great Britain: Clarendon Press Oxford; 1975.
[23] Buttlar W, Bozkurt D, Al-Khateeb G, Waldhoff A. Understanding asphalt mastic behavior through micromechanics. Transportation Research Record: Journal of the Transportation Research Board. 1999(1681):157-69.
[24] Putman BJ, Amirkhanian SN. Characterization of the Interaction Effect of Crumb Rubber Modified Binders Using HP-GPC. Journal of Materials in Civil Engineering. 2010;22(2):153-9.
[25] Yin HM, Buttlar WG, Paulino GH, Benedetto HD. Assessment of Existing Micro-mechanical Models for Asphalt Mastics Considering Viscoelastic Effects. Road Materials and Pavement Design. 2008;9(1):31-57.